Subcritical Statistics in Rupture of Fibrous Materials: Experiments and Model

Stéphane Santucci, Loïc Vanel, and Sergio Ciliberto
Laboratoire de physique, CNRS UMR 5672, Ecole Normale Supérieure de Lyon, 46 allée d'Italie, 69364 Lyon Cedex 07, France
(Received 20 May 2004; published 26 August 2004)

We study experimentally the slow growth of a single crack in a fibrous material and observe stepwise growth dynamics. We model the material as a lattice where the crack is pinned by elastic traps and grows due to thermally activated stress fluctuations. In agreement with experimental data we find that the distribution of step sizes follows subcritical point statistics with a power law (exponent 3/2) and a stress-dependent exponential cutoff diverging at the critical rupture threshold.

DOI: 10.1103/PhysRevLett.93.095505 PACS numbers: 62.20.Mk, 46.50.+a, 81.40.Np

Understanding fracture in solid materials is paramount for a safe engineering design of structures, and many efforts are still needed to obtain a better physical picture. A puzzling observation is the slow rupture of a material when loaded with a *constant external stress* below a critical threshold. Then, the delay time before rupture (or lifetime of the material) strongly depends on the applied stress. Thermodynamics has slowly emerged as a possible framework to describe slow rupture since early experiments have shown temperature dependence of lifetime with an Arrhenius law [1,2]. Statistical physics models assuming perfect elasticity have recently proposed several predictions for lifetime [3–8] as well as for the average dynamics of a slowly growing crack [9]. Efforts are also made to describe slow rupture dynamics from rheological properties of the material such as viscoelasticity and plasticity [10,11].

To be able to distinguish between various theoretical descriptions, more experimental work is needed. We present in this Letter an experiment on slow crack growth in a fibrous material. We have observed that the crack grows by steps of various sizes whose distribution is rather complex and evolves as a function of the crack speed. This behavior can be explained modeling the material as an elastic square lattice where the crack is pinned by elastic traps and adapting the model presented in [9] to describe thermally activated growth of the crack in an energy landscape with multiple metastable states. The model predicts statistical distribution of step sizes in very reasonable agreement with the experiments and has the typical functional form obtained for subcritical point statistics. We stress that the material heterogeneity appears in the model only as a characteristic mesoscopic length scale. The effect of disorder in the material properties and the rheological behavior have not been explicitly included in this simple model.

The experimental system we consider is a two-dimensional sheet with a macroscopic initial crack submitted to a constant load. This geometry is very useful to follow the crack advance using direct observation, while this would be difficult in a three-dimensional geometry because a roughening instability of the crack front line usually occurs. We have used a sheet of fax paper (width $w = 21$ cm, length 24 cm, thickness $e = 50$ μm) for which a natural mesoscopic length scale is the fiber size. Scanning electron microscopy has revealed a size distribution of fibers between 4 and 50 μm, with an average 20 μm. In order to obtain reproducible results, the fax paper was kept in a controlled low level humidity at least one day at $\simeq 10\%$, and also during the experiment at 5%. In these conditions, the paper Young modulus is $Y = 3.5$ GPa. The paper sheet is mounted on a tensile machine with both ends attached with glue tape and rolled several times over rigid tubes. The crack is initiated at the center of the sheet using a calibrated blade. The force F applied to the sample by the tensile machine is measured by a force gage and is perpendicular to the crack direction, which corresponds to a crack opening in a mode I configuration. During an experiment, the crack grows and a feedback mechanism keeps F constant with a precision 0.1 to 0.5 N and a typical time response 10 ms. As a consequence, the stress amplitude at the crack

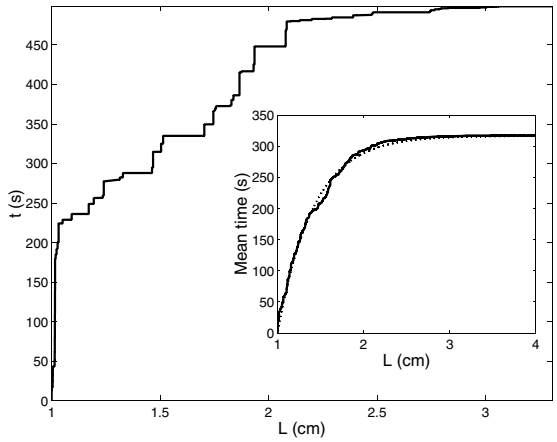

FIG. 1. Time versus crack length for a single experiment showing crack jumps and crack arrest. Inset: The average time to reach L (10 experiments with $F = 270$ N and $L_i = 1$ cm). The dotted curve is obtained from integration of Eq. (1) [9].

 0031-9007/04/93(9)/095505(4)$22.50

tip increases due to stress concentration effects and the motion of the crack accelerates. A high resolution and high speed digital camera (Photron Ultima 1024) is used to follow the crack growth. Image analysis is performed to extract the length of the crack projected on the main direction of propagation. Although the crack actually follows a sinuous trajectory, its projected length gives the main contribution to the stress intensity factor which measures the amplitude of stress divergence near the tip and verifies $K \propto \sigma\sqrt{\ell}$, with σ the external constant stress applied to the sheet and ℓ the projected crack length. The stress σ is estimated from F and the area A of a cross section of the sheet, A being approximatively constant: $\sigma = F/A$. Because of the small thickness of the paper a slight buckling occurs, but it has been shown that the scaling with stress and crack length is not significantly modified [12]. On the other hand, finite width corrections on the stress intensity factor have been taken into account: $K = g(\ell/w)\sigma\sqrt{\ell}$ with $g(\ell/w) = [(w/\ell)\tan(\pi\ell/2w)]^{1/2}$ [13].

A typical growth curve is shown in Fig. 1. It clearly appears that the crack does not grow smoothly: essentially, there are periods of rest where the crack tip does not move and periods where it suddenly opens and advances of a certain step size s. We have extensively studied the growth varying the initial crack length ($1 < \ell_i < 4$ cm) and the applied force ($140 < F < 280$ N), equivalent to an initial stress intensity factor K_i between 2.7 and 4.2 MPa m$^{1/2}$. The resulting measured lifetime varied from a few seconds to a few days depending on the value of the applied stress or the temperature. Even for the same experimental conditions (same stress, initial crack length, and temperature) a strong dispersion in lifetime was observed as expected in a model of thermally activated growth [9]. Furthermore, the average growth dynamics shows an exponential approach of lifetime in good agreement with the model (see inset) [9]. Results from the average dynamics are detailed elsewhere. Here, we want to study more extensively the step size statistics.

It is commonly observed that the crack velocity is an increasing function of the stress intensity factor K. Thus, it is natural to look at the step statistics for a given value of K. In practice, the step size distributions have been obtained for various ranges of K. Figure 2 shows the step size distributions determined from all the data we have collected using a logarithmic binning. Typically, 700 data points are used to obtain each distribution. Two regimes are observed. For small step sizes, the distribution does not depend on the value of K, while for larger step sizes there is a cutoff size increasing with K. In practice, the toughness of the material, i.e., its critical stress intensity factor $K_c = 6.5 \pm 0.05$ MPa m$^{1/2}$, has been obtained as the value of K beyond which the probability to detect a jump vanishes.

The behavior observed for the step size distributions can be predicted using minimal physical properties. Let us assume that the material is mainly elastic but that there is a scale at which the material becomes discontinuous. In a perfect crystal, the only such scale would be the atomic scale, but in a fibrous material like paper, we have an intermediate mesoscopic scale, the typical fiber size. The elastic description of a material at a discrete level leads to a lattice trapping effect [14] with an energy barrier that has been estimated analytically [15]. To get a physical picture of the trapping in our geometry, we have modeled numerically a 2D square lattice of linear springs where the crack corresponds to a given number of adjacent broken springs as described in [9]. The lattice is loaded with a constant force, and we estimate the minimum increase in potential energy needed to bring the first spring at the crack tip at the breaking threshold. This energy is obtained by applying an external force on the spring at the crack tip and computing the change in

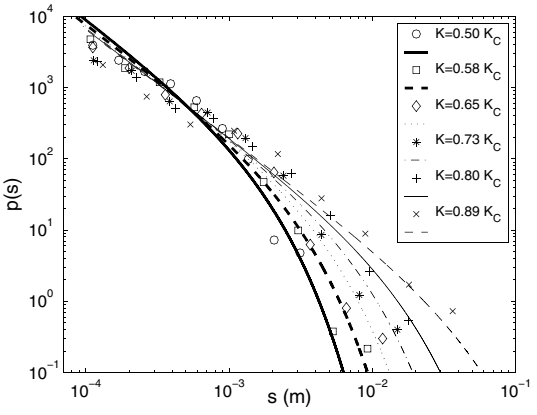

FIG. 2. Probability distribution of step sizes for various values of stress intensity factor. Choosing $\lambda = 50$ μm, the different curves are the best fits of Eq. (3) giving an average value $V = 5 \pm 1$ Å^3.

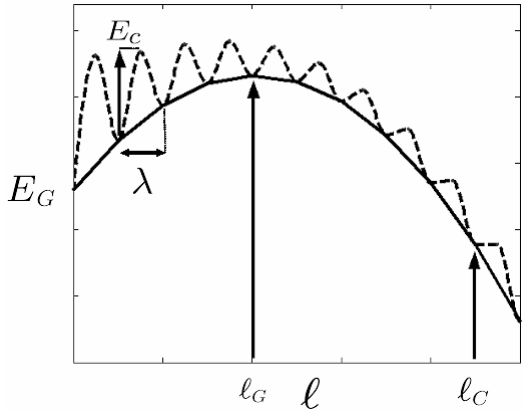

FIG. 3. Sketch of the Griffith potential energy E_G as a function of crack length ℓ with constant applied stress (solid line). The energy barriers E_C and the discretization scale λ are represented by the dashed curve.

elastic energy of the whole lattice as well as the work done by the constant force at the boundaries. We find an energy barrier per unit volume: $E_c \simeq (\sigma_c - \sigma_m)^2/2Y$, where Y is the Young modulus, σ_c the material stress threshold for rupture, and $\sigma_m (< \sigma_c)$ the equilibrium local stress at the crack tip estimated at the discrete scale λ, i.e., $\sigma_m = K/\sqrt{\lambda}$. To each position of the crack tip corresponds a different value of the energy barrier since the stress at the tip increases with the crack length. Once the spring breaks, the crack moves by at least one lattice spacing λ. The equilibrium potential energy of the whole system is given by the Griffith energy per unit thickness of the sheet [16]: $E_G = E_0 - \pi \ell^2 \sigma^2/4Y + 2\gamma\ell$, where γ is the surface energy. In Fig. 3 we schematically represent the energy barrier of trapping and the Griffith energy. In agreement with a previous analysis [15], we find that the crack length ℓ_c at which the energy barrier becomes zero is about twice the Griffith length ℓ_G where the equilibrium potential energy reaches its maximal value.

In order to model crack rupture as a thermally activated process, we recall first ideas that were presented in [9]. Because of thermal noise at finite temperature T in a fixed volume V, there are statistical stress fluctuations σ_f around the equilibrium value σ_m with a Gaussian distribution: $p(\sigma_f) \propto \exp[-(\sigma_f - \sigma_m)^2 V/2Yk_BT]$. The material will break if the stress fluctuation σ_f becomes larger than the threshold σ_c with a probability: $P(\sigma_f > \sigma_c) = \int_{\sigma_c}^{\infty} p(\sigma_f) d\sigma_f$. Assuming the rupture process is irreversible, the velocity v of the crack tip is set proportional to the probability $P(\sigma_f > \sigma_c)$ which gives

$$v = \frac{\lambda}{\tau_0} \int_{U_c}^{\infty} \frac{e^{-U_f} dU_f}{\sqrt{\pi U_f}}, \tag{1}$$

where $U_f = (\sigma_f - \sigma_m)^2 V/2Yk_BT$, $U_c = U_f(\sigma_f = \sigma_c)$, and τ_0 is an elementary time scale (typically, an inverse vibrational frequency). Integration of Eq. (1) gives the average growth curve in inset of Fig. 1.

We extend now this model to describe thermally activated and irreversible motion of a crack in the rugged potential energy landscape introduced above. Below ℓ_c, the energy barriers $E_c(\sigma_m)$ trap the crack in a metastable state for an average time τ_p depending on the barrier height. Irreversible crack growth is a very reasonable assumption when $\ell > \ell_G$ since the decrease in equilibrium potential energy makes it more likely for the crack to open than to close. When a fluctuation σ_f occurs, it increases locally the free energy per unit volume by $E_f(\sigma_m) \simeq (\sigma_f - \sigma_m)^2/2Y$ (this comes from a Taylor expansion of the bulk elastic free energy in agreement with the numerical estimate of E_c and the Gaussian form of the stress fluctuations). The energy E_f can be used by the crack to overcome the barrier. If there are no dissipative mechanisms, the crack will grow indefinitely when $\ell > \ell_G$ as the barriers get smaller and smaller and the release of elastic energy helps to reach a more energetically favorable position. We introduce a simple mechanism of crack arrest assuming that after overcoming the energy barrier the crack loses an energy identical to the barrier size and does not gain any momentum from the elastic release of energy (experimentally, dissipation comes from acoustic wave emissions, viscous or plastic flow, etc.). When the crack reaches the next trap, it still has an energy $E_f - E_c$ which might be sufficient to overcome the next barrier. For a given fluctuation energy E_f, the crack typically has enough energy to overcome a number of barriers $n = E_f(\sigma_m)/E_c(\sigma_m)$ and makes a jump of size $s = n\lambda$ [the decrease of $E_c(\sigma_m)$ with σ_m during a jump of size s has been neglected]. The probability distribution for E_f is explored at each elementary step τ_0, while the probability distribution of step size is explored after each average time τ_p spent in the trap. In order to relate the two probabilities, we express the mean velocity in a different way as the ratio of the average step size to the average trapping time:

$$v = \frac{\int_{\lambda}^{\infty} s p(s) ds}{\tau_p}. \tag{2}$$

From the identity between Eqs. (1) and (2), and the normalization condition of the probability [$\int_{\lambda}^{\infty} p(s) ds = 1$], we obtain the probability distribution:

$$p(s) = N(U_c) \frac{\sqrt{\lambda} e^{-s/\xi}}{2s^{3/2}}, \tag{3}$$

where $N(U_c) = [e^{-U_c} - \sqrt{\pi U_c}\,\mathrm{erfc}(\sqrt{U_c})]^{-1}$ and $\xi = \lambda/U_c$. We find a power law with an exponent $3/2$ and an exponential cutoff with a characteristic length $\xi \sim (\sigma_c - \sigma_m)^{-2}$ diverging at the critical stress σ_c. Incidently, we note that this probability has a form similar to subcritical point probability distributions in percolation theory [17]. From Eq. (3), we can compute from this distribution the first and second order moments:

$$\langle s \rangle = N(U_c) \frac{\lambda\sqrt{\pi}}{2\sqrt{U_c}} \mathrm{erfc}(\sqrt{U_c}), \tag{4}$$

$$\langle s^2 \rangle = N(U_c) \frac{\lambda^2\sqrt{\pi}}{4U_c^{3/2}} \left(\mathrm{erfc}(\sqrt{U_c}) + 2\sqrt{\frac{U_c}{\pi}} e^{-U_c} \right). \tag{5}$$

We obtain two asymptotical behaviors. When the relative energy barrier is high ($U_c \gg 1$), $\langle s \rangle \simeq \lambda$ and $\langle s^2 \rangle \simeq \lambda^2$. In this limit, there is only one step size possible. When the relative energy barrier becomes low ($U_c \ll 1$), we predict a divergence at critical point: $\langle s \rangle \sim (\sigma_c - \sigma_m)^{-1}$ and $\langle s^2 \rangle \sim (\sigma_c - \sigma_m)^{-3}$. Then, the crack velocity is expected to be dominated by the critical divergence of crack jumps.

To compare with our experimental data, we use an estimate of the stress near the crack tip by assuming as above that $\sigma_m = K/\sqrt{\lambda}$. In addition, the normalization

condition of the distribution actually reduces the model to one parameter, the ratio V/λ^2. In our model, λ represents the mesoscopic scale of discretization in paper. Setting $\lambda = 50\ \mu$m, V is the only unknown. One parameter fits of step size distributions in Fig. 2 for each range of stress intensity factors give very robust results: $V = 5 \pm 1$ Å^3. To check the asymptotic limit close to the critical point, we have plotted in Fig. 4 $\langle s \rangle$ and $\langle s^2 \rangle^{1/3}$ as a function of $K_c/(K_c - K_m)$. Here, the first and second order moments have been computed from the raw measurements in a given range of K. Because it requires less statistics to estimate the first two moments of the distribution than the distribution itself, we are able to narrow the width of the K range for each data point without changing the global trend. The solid lines represent the model prediction using the fitted value of V from the distributions of Fig. 2. Not only does the model reproduce reasonably well the evolution of the step size distributions with σ_m (V is essentially constant and all the other parameters are fixed), but the asymptotic divergence of the first two moments of the distribution are also well reproduced. For the mean step size, the scaling is observed up to K values very close to K_c (1%). In the model, we see that the ratio of the second order moment over the first order moment is diverging at K_c. Thus, close to K_c, the second order moment becomes more inaccurate than the measure of the mean.

The value obtained for the volume V is at the atomic scale ($V^{1/3} \simeq 1.7$ Å). Its small value gives an idea of the microscopic scale at which the thermodynamical stress fluctuations have the proper amplitude to trigger rupture in our model. It should be realized that the model actually predicts a lower limit for this microscopic scale. First, it assumes a strong dissipation of energy during crack advance since none of the elastic release of energy is used to keep the crack moving. This is certainly an overestimation of a real dissipative mechanism, would it be viscoelastic or plastic. Decreasing dissipation in the model permits larger steps of the crack. In order to obtain the same experimental velocity, the trapping time must also be larger which will happen if the rupture occurs at a larger microscopic scale. Second, disorder in the material properties has been completely neglected. It has been shown recently that disorder effectively reduces the energy cost for breaking, and this also permits rupture at a larger microscopic scale [8]. Further theoretical work needs to be done to introduce a more realistic dissipative mechanism and takes into account disorder in the material properties. As the model stands now, we believe that it should apply to any elastic materials for which a structure at a mesoscopic scale exists. For example, it would be interesting to understand if the model can explain crack jump dynamics observed in semicrystalline polymers [18]. To conclude, we have shown that a simple model of thermally activated crack dynamics is able to reproduce with good accuracy the step size distribution of the crack growth. This is quite interesting because it may open new perspectives in the description of rupture as a thermally activated process.

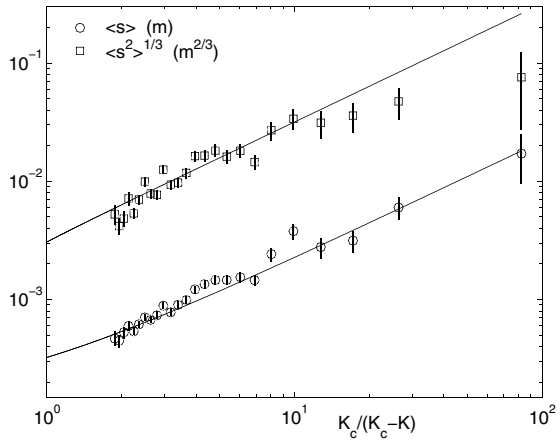

FIG. 4. The mean and cubic root of the second order moment of step sizes is well reproduced by the model [Eqs. (4) and (5)] plotted with $\lambda = 50\ \mu$m and $V = 5$ Å^3.

We acknowledge illuminating discussions with E. Bouchaud, J.-P. Bouchaud, M. Ciccotti, and M. Marder.

[1] S. S. Brenner, J. Appl. Phys. **33**, 33 (1962).
[2] S. N. Zhurkov, Int. J. Fract. Mech. **1**, 311 (1965).
[3] L. Golubovic and S. Feng, Phys. Rev. A **43**, 5223 (1991).
[4] Y. Pomeau, C.R. Acad. Sci. Paris II **314**, 553 (1992).
[5] A. Buchel and J. P. Sethna, Phys. Rev. Lett. **77**, 1520 (1996); Phys. Rev. E **55**, 7669 (1997).
[6] K. Kitamura, I. L. Maksimov, and K. Nishioka, Philos. Mag. Lett. **75**, 343 (1997).
[7] S. Roux, Phys. Rev. E **62**, 6164 (2000).
[8] R. Scorretti, S. Ciliberto, and A. Guarino, Europhys. Lett. **55**, 626 (2001); Physica (Amsterdam) **158D**, 83 (2001).
[9] S. Santucci, L. Vanel, R. Scorretti, A. Guarino, and S. Ciliberto, Europhys. Lett. **62**, 320 (2003).
[10] J. S. Langer, Phys. Rev. Lett. **70**, 3592 (1993).
[11] A. Chudnovsky and Y. Shulkin, Int. J. Fract. **97**, 83 (1999).
[12] E. Riks, C. C. Rankin, and F. A. Brogan, Eng. Fract. Mech. **43**, 529 (1992).
[13] B. R. Lawn and T. R. Wilshaw, *Fracture of Brittle Solids* (Cambridge University Press, Cambridge, 1975).
[14] R. Thomson, Solid State Phys. **39**, 1 (1986).
[15] M. Marder, Phys. Rev. E **54**, 3442 (1996).
[16] A. A. Griffith, Philos. Trans. R. Soc. London A **221**, 163 (1920).
[17] D. Stauffer, *Introduction to Percolation Theory* (Taylor & Francis, London, 1991).
[18] M. Parsons, E.V. Stepanov, A. Hiltner, and E. Baer, J. Mater. Sci. **34**, 3315 (1999); **35**, 2659 (2000).